

J.A. Tenreiro Machado · Béla Pátkai
Imre J. Rudas *Editors*

Intelligent Engineering Systems and Computational Cybernetics

 Springer

Robotic Manipulators with Vibrations: Short Time Fourier Transform of Fractional Spectra

Miguel F. M. Lima¹, J. A. Tenreiro Machado², and Manuel Crisóstomo³

¹ Dept. of Electrotechnical Engineering, Superior School of Technology, Polytechnic Institute of Viseu, 3504-510 Viseu, Portugal

lima@mail.estv.ipv.pt

² Dept. of Electrotechnical Engineering, Institute of Engineering, Polytechnic Institute of Porto, 4200-072 Porto, Portugal

jtm@isep.ipp.pt

³ Instituto de Sistemas e Robótica, Department of Electrical and Computer Engineering, University of Coimbra, Polo II, 3030-290 Coimbra, Portugal

mcris@isr.uc.pt

Summary. This paper analyzes the signals captured during impacts and vibrations of a mechanical manipulator. In order to acquire and study the signals an experimental setup is implemented. The signals are treated through signal processing tools such as the fast Fourier transform and the short time Fourier transform. The results show that the Fourier spectrum of several signals presents a non integer behavior. The experimental study provides valuable results that can assist in the design of a control system to deal with the unwanted effects of vibrations.

1 Introduction

In practice the robotic manipulators present some degree of unwanted vibrations. In fact, the advent of lightweight arm manipulators, mainly in the aerospace industry, where weight is an important issue, leads to the problem of intense vibrations. On the other hand, robots interacting with the environment often generate impacts that propagate through the mechanical structure and produce also vibrations.

Motivated by the problem of vibrations, this paper studies the robotic signals captured during an impact phase of the manipulator. The study is done in a fractional calculus (FC) perspective. In order to analyze the phenomena involved an acquisition system was developed. The manipulator motion produces vibrations, either from the structural modes or from end-effector impacts. The instrumentation system acquires signals from multiple sensors that capture the axis positions, mass accelerations, forces and moments and electrical currents in the motors. Afterwards, an analysis package, running off-line, reads the data recorded by the acquisition system and examines them. Bearing these ideas in mind, this paper is organized as follows. Section 2 addresses the motivation for this work. Section 3 describes briefly the

robotic system enhanced with the instrumentation setup. Section 4 presents the experimental results. Finally, Section 5 draws the main conclusions and points out future work.

2 Motivation

Reference [15] mentions several techniques for reducing vibrations and its implementation either at the robot manufacturing stage or at the operational stage. Briefly, the techniques can be enumerate as: (i) conventional compensation, (ii) structural damping or passive vibration absorption, (iii) control based on the direct measurement of the absolute position of the gripper, (iv) control schemes using the direct measurement of the modal response, (v) active control, driving out energy of the vibration modes, (vi) use a micromanipulator at the endpoint of the larger manipulator and (vii) adjustment of the manipulator command inputs so that vibrations are eliminated.

The work presented here is a step towards the implementation of the sixth technique. In recent years the use of micro/macro robotic manipulators has been proposed for space applications and nuclear waste cleanup. Several authors have studied this technique [16], namely [4, 11] that adopted a command filtering approach in order to position the micromanipulator. Also, [4, 6] used inertial damping techniques taking advantage of a micro manipulator located at the end of a flexible link.

The experiments described in this paper use a macro manipulator, with a low bandwidth, that is compensated through a much faster micromanipulator inserted at the robot endpoint. In this perspective, in order to eliminate or reduce the effect of the vibration is fundamental to study variables, for implementing an adequate control of the macro/micro system.

Bearing these ideas in mind, is presented a study of the robotic signals, in a FC perspective. In fact, the study of feedback fractional order systems has been receiving considerable attention [9, 10] due to the facts that many physical systems are well characterized by fractional-order models [14]. With the success in the synthesis of real noninteger differentiator and the emergence of new electrical circuit element called “fractance” [3], and fractional-order controllers [2], have been designed and applied to control a variety of dynamical processes [13]. Therefore the study presented here can assist in the design of the control system to be used.

3 Experimental Platform

The developed experimental platform has two main parts: the hardware and the software components [7]. The hardware architecture is shown in Fig. 1. Essentially it is made up of a robot manipulator, a Personal Computer (PC) and an interface electronic system. The interface box is inserted between the robot arm and the robot controller, in order to acquire the internal robot signals; nevertheless, the interface captures also external signals, such as those arising from accelerometers and force/torque sensors, and controls the external micro-arm. The modules are made up of electronic cards specifically designed for this work. The function of the modules is to adapt the signals and to isolate galvanically the robot’s electronic equipment from the rest of the hardware required by the experiments.

The software package runs in a Pentium 4, 3.0 GHz PC and, from the user’s point of view, consists of two applications:

- The acquisition application is a real time program responsible for acquiring and recording the robot signals.

- The analysis package runs off-line and handles the recorded data. This program allows several signal processing algorithms such as, Fourier transform (FT), correlation, time synchronization, etc.

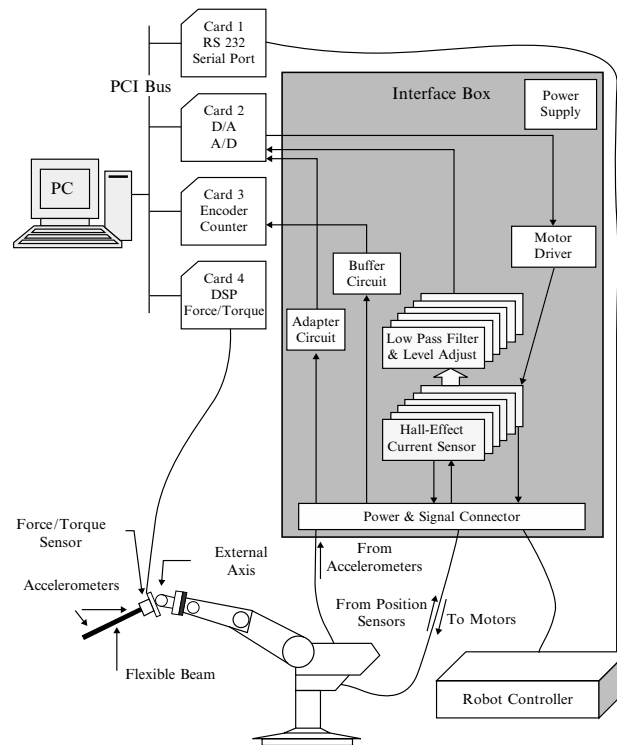


Fig. 1: Block diagram of the hardware architecture

4 Experimental Results

In the experiment is used a steel rod flexible link. To test impacts, the link consists of a long, thin, round, flexible steel rod clamped to the end-effector of the manipulator. The robot motion is programmed in a way such that the rod moves against a rigid surface. Figure 2 depicts the robot with the flexible link and the impact surface. The physical properties of the flexible beam are shown in Table 1.

During the motion of the manipulator the clamped rod is moved by the robot against a rigid surface. An impact occurs and several signals are recorded with a sampling frequency of $f_s = 500$ Hz. The signals come from different sensors, such as accelerometers, force and torque sensor, position encoders and current sensors.

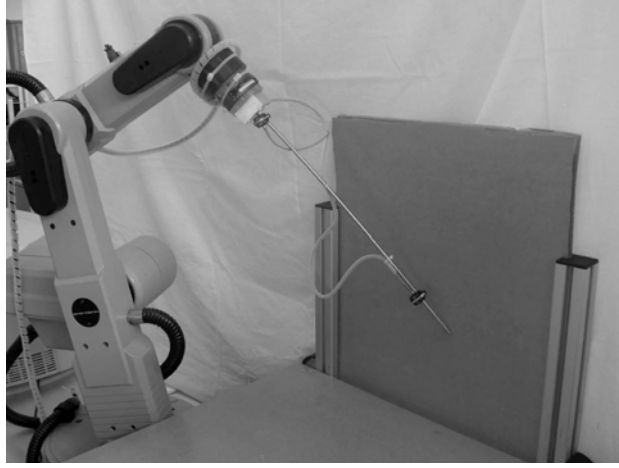


Fig. 2: Steel rod impact against a rigid surface.

Table 1: Physical properties of the flexible beam

Characteristic	Steel rod
Density (kg m^{-3})	7.86×10^3
Elasticity modulus (N m^{-2})	200×10^9
Mass (kg)	0.107
Length (m)	0.475
Diameter (m)	5.75×10^{-3}

4.1 Time Domain

A typical time evolution of some variables is shown in Figs. 3–4 corresponding to: (i) the impact of the rod on a rigid surface and (ii) without impact [8].

In this example, the signals present clearly a strong variation at the instant of the impact that occurs, approximately, at $t = 4$ sec. Consequently, the effect of the impact force, shown in Fig. 4 (left), is reflected in the current required by the robot motors (see Fig. 3, left). Figure 4 (right) shows the accelerations at the rod free-end (accelerometer 1), where the impact occurs, and at the rod clamped-end (accelerometer 2). The amplitudes of the accelerometers signals are higher near the rod impact side. The two signals are superimposed in Fig. 4 (right). The first acceleration peak (accelerometer 1), due to the impact, corresponds to the rigid surface (case *i*) while the second peak corresponds to the care of no impact (case *ii*).

4.2 Fourier Transform

In order to study the behavior of the signal FT, a trendline can be superimposed over the spectrum. The trendline is based on a power law approximation:

$$|\mathcal{F}\{f(t)\}| \approx c\omega^m \quad (1)$$

where \mathcal{F} is the signal FT, $c \in \mathfrak{R}$ is a constant that depends on the amplitude, ω is the frequency and $m \in \mathfrak{R}$ is the slope.

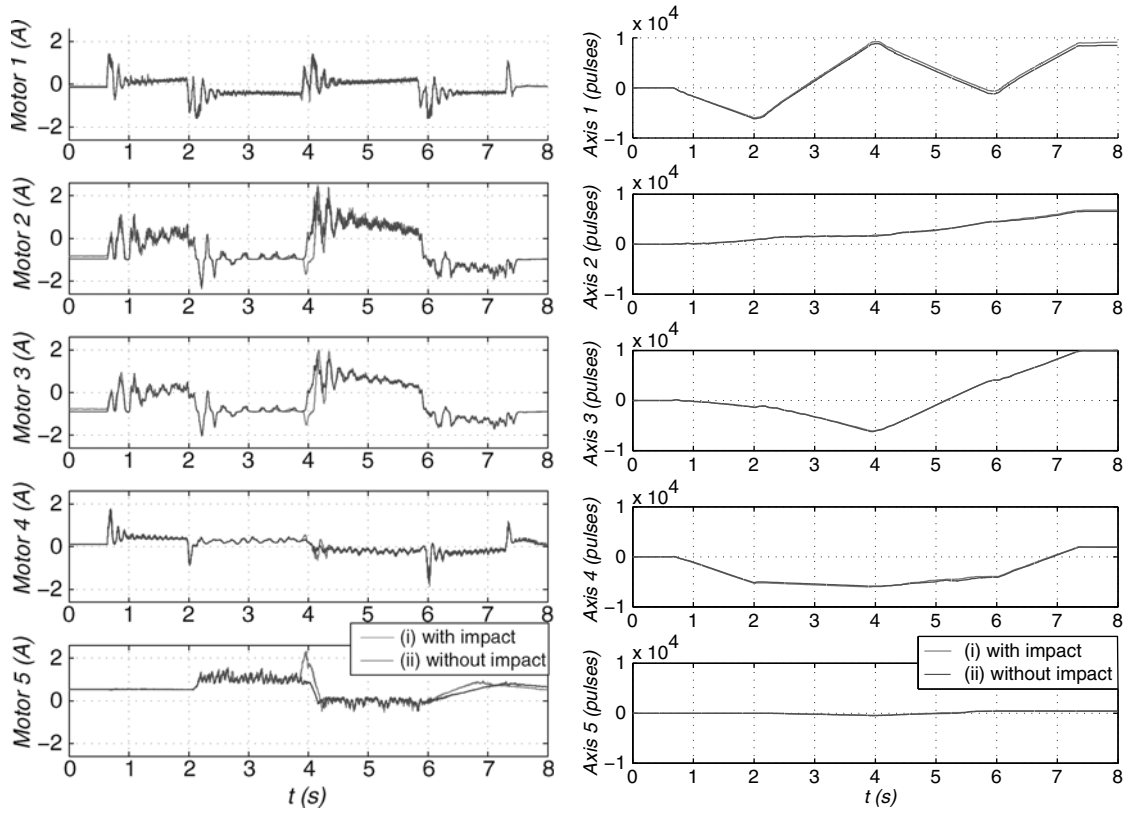


Fig. 3: Electrical currents of robot axis motors (left) and robot axis positions (right)

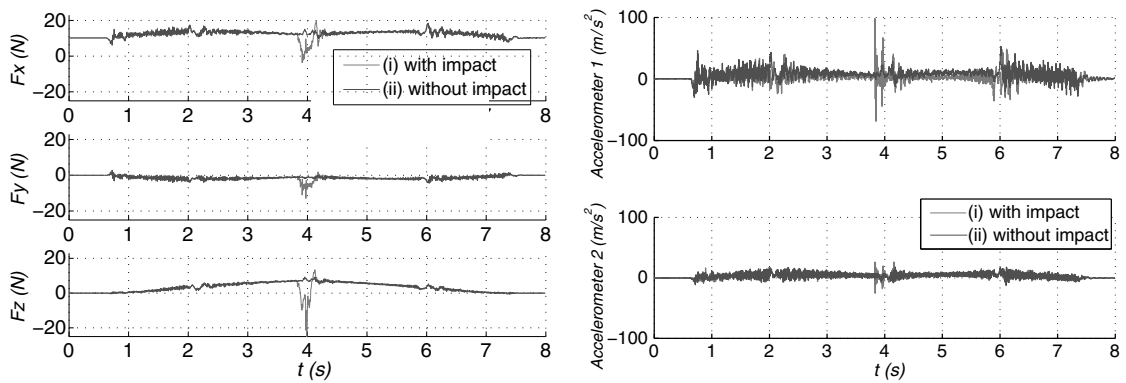


Fig. 4: Forces at the gripper sensor (left) and rod accelerations (right)

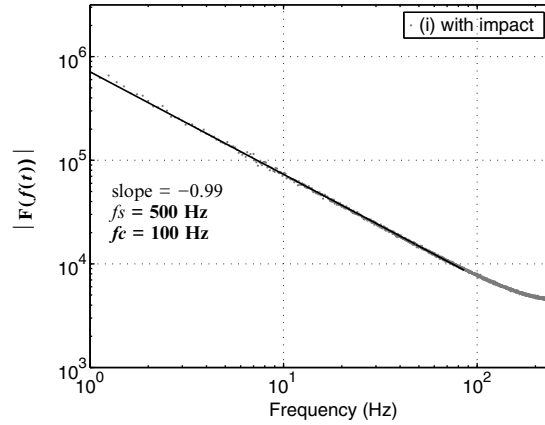


Fig. 5: Spectrum of the axis 1 position

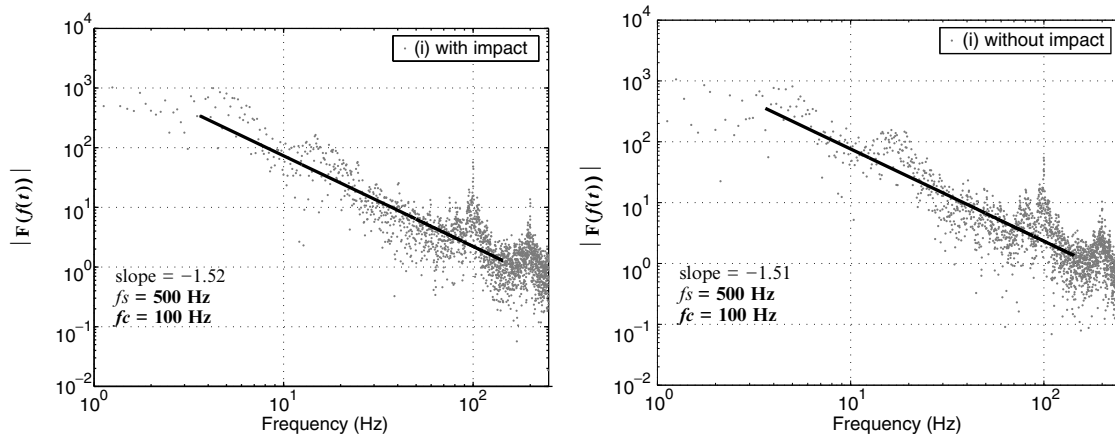


Fig. 6: Spectrum of the axis 3 motor current

Figure 5 shows the amplitude of the Fast Fourier Transform (FFT) of the axis 1 position signal. The trendline (1) leads to a slope $m = -0.99$ revealing, clearly, the integer order behavior. The others position signals were studied, revealing also an integer behavior, both under impact and no impact conditions. Figure 6 shows the amplitude of the FFT of the electrical current for the axis 3 motor. The spectrum was also approximated by trendlines in a frequency range larger than one decade. These trendlines (Fig. 6) have slopes of $m = -1.52$ and $m = -1.51$ under impact (i) and without impact (ii) conditions, respectively. The lines present a fractional order behavior in both cases. Figure 7 depicts the amplitude of the FFT of the electrical current for the axis 4 motor. Here the trendlines present slopes that vary slightly (slopes $m = -1.58$ with impact and $m = -1.64$ without impact) but, in both cases, continue to reveal a fractional order behavior. The others axis motor currents were studied, as well. Some of them, for a limited frequency range, present also fractional order behavior while others have a complicated spectrum difficult to approximate by one trendline. According to the robot manufacturer specifications the loop control of the robot has a cycle time of $t_c = 10$ mSec. This

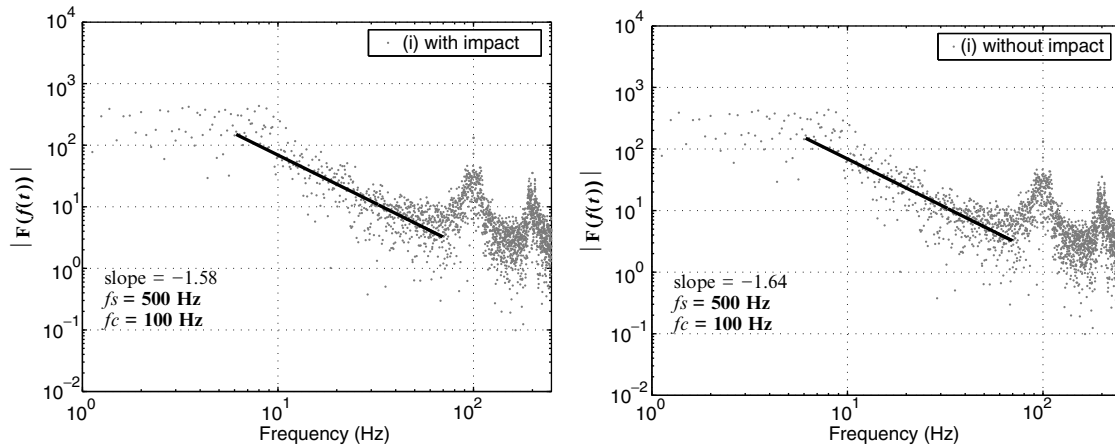
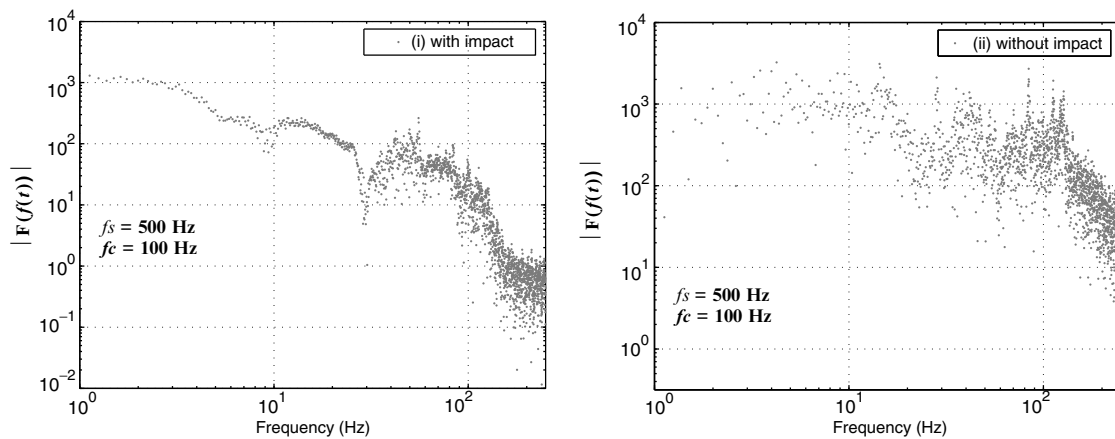


Fig. 7: Spectrum of the axis 4 motor current


 Fig. 8: F_z force spectrum with impact (left) and acceleration spectrum of the rod free-end without impact (right)

fact is observed approximately at the fundamental ($f_c = 100$ Hz) and multiple harmonics in all spectra of motor currents (Figs. 6 and 7). Figure 8 (left) shows, as example, the spectrum of the F_z force. This spectrum is not so well defined in a large frequency range. All force/moments spectra present identical behavior and, therefore, it is difficult to define accurately the behavior of the signals. Finally, Fig. 8 (right) depicts the spectrum of the signal captured from the accelerometer 1 located at the rod free-end of the beam.

Like the spectrum from the other accelerometer, this spectrum is spread and complicated. Therefore, it is difficult to define accurately the slope of the signal and consequently its behavior in terms of integer or fractional system.

4.3 Short Time Fourier Transform

Several spectra of the signals captured during approximately 8 sec are represented in Figs. 5–8. The signal spectra are scattered and, therefore, in order to obtain smoother curves is used a multiwindow algorithm. If we time slice the signals and calculate the Fourier transform, then for each obtained section of the signal, the resulting spectrum is a smoother curve. One way of obtaining the time-dependent frequency content of a signal is to take the Fourier transform of a function over an interval around an instant τ , where τ is a variable parameter [5]. The Gabor Transform accomplishes this by using the Gaussian window. The short time Fourier transform (STFT), also known as windowed Fourier transform (WFT), generalizes the Gabor transform by allowing a general window function [1]. The concept of this mathematical tool is very simple. We multiply $x(t)$, which is the signal to be analyzed, by an analysis moving window $x(t)g(t - \tau)$, and then we compute the Fourier transform of the windowed signal $x(t)g(t - \tau)$. Each FT gives a frequency domain ‘slice’ associated with the time value at the window centre. Actually, windowing the signal improves local spectral estimates [12]. Considering the window function centered at time τ , the STFT is represented analytically by:

$$F_w(\tau, \omega) = \int_{-\infty}^{+\infty} x(t)w(t - \tau)e^{-j\omega t} dt \quad (2)$$

where $\omega = 2\pi f$ is the frequency.

Each window has a width of t_w , where $t_{min} < t_w < t_{max}$ and the time between the centers of two successive windows is δ . Therefore, the frequencies of the analyzing signal $f < 1/t_w$ are rejected by the STFT. Diminishing t_w produces a reduction of the frequency resolution and an increase in the time resolution. Augmenting t_w has the opposite effect. Therefore, the choice of the STFT window entails a well-known duration-bandwidth tradeoff.

On the other hand, the window can introduce an unwanted side effect in the frequency domain. As a result of having abrupt truncations at the ends of the time domain caused by the window, specially the rectangular one, the spectrum of the FT will include unwanted “side lobes”. This gives rise to an oscillatory behavior in the FT results called the Gibbs Phenomenon [12]. In order to reduce this unwanted effect, generally is used a weighting window function that attenuate signals at their discontinuities. For that reason there are several others popular windows normally adopted in the STFT, namely, Hanning, Hamming, Gaussian, Blackman, etc.

In this line of thought, several experiments were developed with different windows shapes. Due to space limitations we are only depicting the more relevant features. In Fig. 9 are shown the spectra versus time of the axis 4 motor current, using a STFT with rectangular, Hamming, Gaussian and Hanning window, respectively. The STFT with the rectangular window presents clearly the Gibbs Phenomenon. The tests show that the STFT with the Hamming window present also this phenomenon, though to a smaller extend. The STFTs with the Hanning, Blackman and Gaussian windows present the best behavior, with slightly differences. Therefore, in the experiments described we adopt the rectangular, Hamming, Gaussian and Hanning windows. The adequate time parameters of the window, namely the width (t_w) and the inter-spacing time (δ) for the STFT were determined by trial and error. Figure 10 depicts the amplitude of the FFT of the electrical current for the axis 4 motor under impact condition using a Gaussian window for $\tau = 2$ sec. In this example the trendline presents a slope of approximately $m = -1.89$. According with the position in time of the moving window, the slope of the trendline will varies revealing different spectral component along the acquisition time.

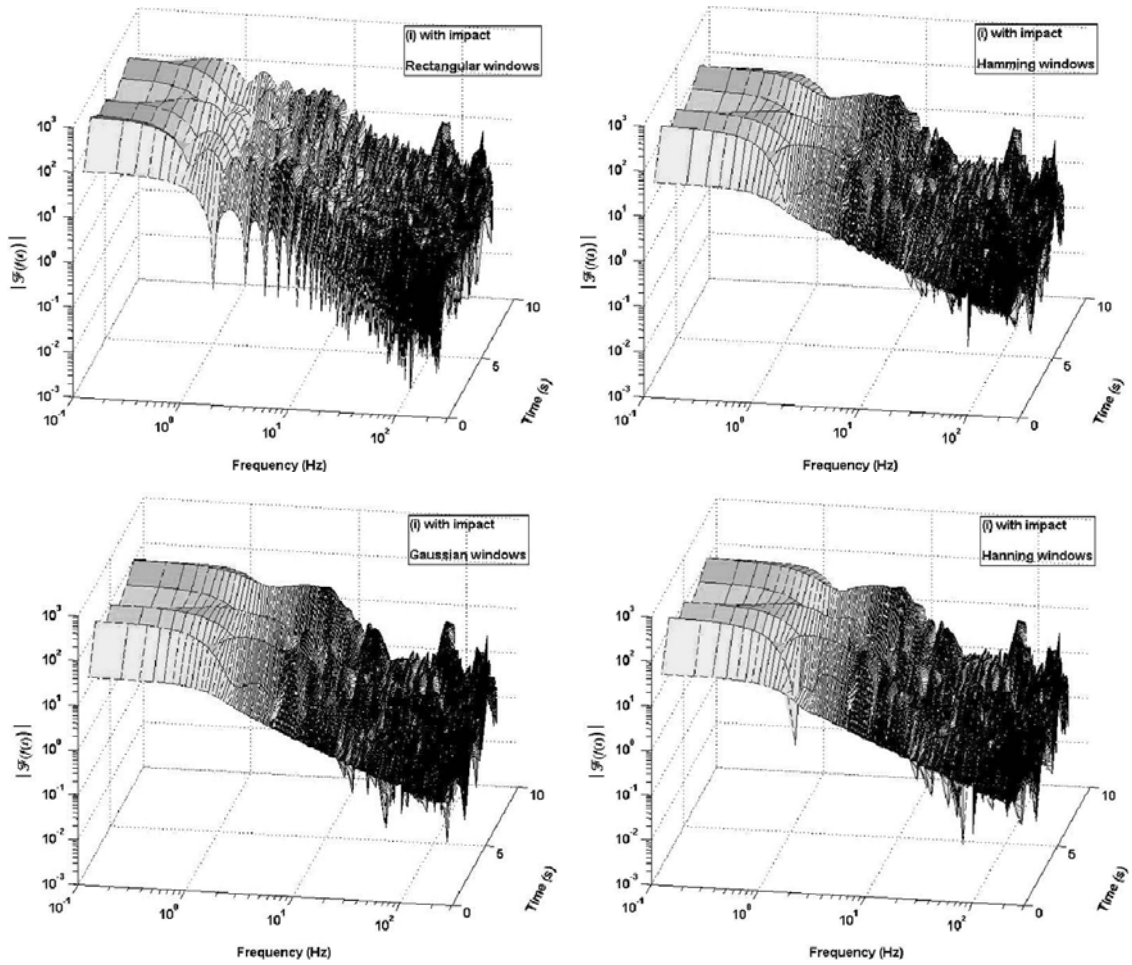


Fig. 9: STFT of axis 4 motor current using the window {rectangular, Hamming, Gaussian, Hanning}, for $\delta = 1$ (sec) and $t_w = 1$ (sec)

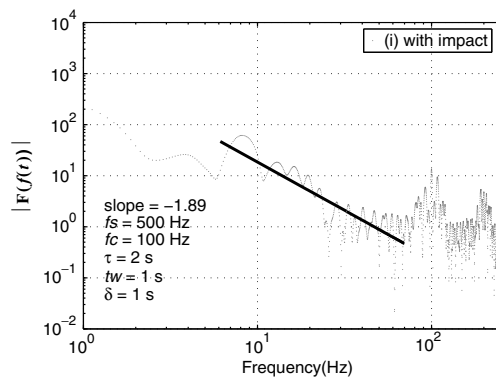


Fig. 10: Spectrum of the axis 4 motor current using a Gaussian window

This fact can be seen in Fig. 11. These figures shows the calculated slope for the spectrum obtained applying Rectangular, Gaussian and Hanning windows with different widths t_w . The inter-space time of two successive windows consists of $\delta = 1$ sec.

The wider the window of time, the closer the value of the slope of each window is to the slope calculated by the classical FT, as would be expected. From Fig. 11 it can be seen that a STFT using a window length of $t_w = 0.25$ sec presents a kind of an erratic behavior, showing therefore that is an unsuitable window.

Moreover, in Fig. 11 it can be seen the different behavior of the slopes obtained by the rectangular window comparing with the Gaussian and Hanning windows. Actually, as referred before, using the rectangular window the several slopes present an erratic behavior caused by the Gibbs phenomena.

On the other hand, the slopes obtained by the Gaussian and Hanning windows with suitable parameters, namely, $t_w = \{0.5, 1, 2, 4\}$, are similar, which shows the best behavior of these windows.

We tried the same approach to others acquisitions from the same signal (the axis 4 motor current) at identical conditions. The conclusions were almost identical, which reveals the consistent results presented here.

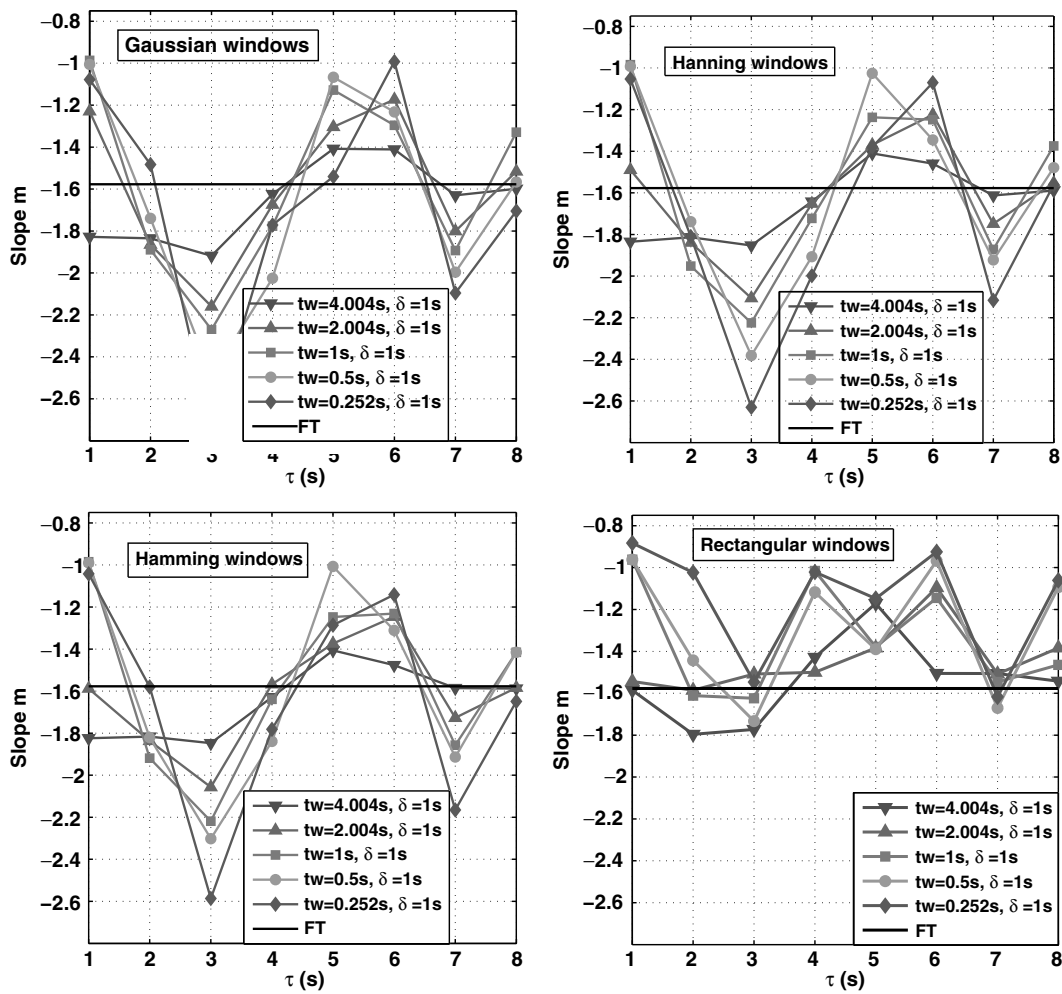


Fig. 11: Slopes of the spectrum of the axis 4 motor current under impact condition using {Gaussian, Hanning, Hamming, rectangular} windows with $t_w = \{0.25, 0.5, 1, 2, 4\}$ (sec) and $\delta = 1$ (sec)

5 Conclusions

In this paper an experimental study of several robot signals was presented. The study was done in a FC perspective and the use of the STFT confirms the fractional nature of the signals whose behavior was analyzed by the classical FT also. This study provides useful information that can assist in the design of a control system to be used in eliminating or reducing the effect of vibrations.

The next stage of development of the software and hardware apparatus is to reduce the vibrations and its effect upon the robot structure. In this line of thought, is under development a micromanipulator, with a higher frequency response than the main manipulator, mounted at the end-effector and actively counter-acting the undesirable dynamics.

References

1. Allen R L, Mills D W (2004) *Signal Analysis*. Wiley-Interscience, New York
2. Barbosa R S, Tenreiro Machado J A, Ferreira I M (2005) Tuning of pid controllers based on Bode's ideal transfer function. In: *Nonlinear Dynamics*, pp 305–321. Kluwer, Netherlands.
3. Bohannan G W (2002) Analog realization of a fractional control element – revisited. In: mechatronics.ece.usu.edu/foc/cdc02tw/cdrom/additional/FOC_Proposal_Bohannan.pdf
4. Cannon D W, Magee D P, Book W J, Lew J Y (1996) Experimental study on micro/macro manipulator vibration control. In: *Proceedings of the IEEE International Conference on Robotics & Automation*. Minneapolis, Minnesota, USA.
5. Gabor D (1946) Theory of communication. *J. IEE*, 93:429–457, 1946.
6. Lew J Y, Trudnowski D J, Evans M S, Bennett D W (1995) Micro-manipulator motion control to suppress macro-manipulator structural vibrations. In: *Proceedings of the IEEE International Conference on Robotics & Automation*, Nagoya, Japan, pp 3116–3120.
7. Lima M F M, Tenreiro Machado J A, Crisóstomo M (2005) Experimental set-up for vibration and impact analysis in robotics. *WSEAS Transactions on Systems* 4(5):569–576
8. Lima M F M, Tenreiro Machado J A, Crisóstomo M (2006) Fractional order Fourier spectra in robotic manipulators with vibrations. In: *Second IFAC Workshop on Fractional Differentiation and Its Applications*, Porto, Portugal, pp 386–391
9. Tenreiro Machado J A (1997) Analysis and design of fractional-order digital control systems. *Journal of Systems Analysis-Modelling-Simulation* 27:107–122
10. Tenreiro Machado J A (2003) A probabilistic interpretation of the fractional-order differentiation. *Journal of Fractional Calculus & Applied Analysis* 6:73–80
11. Magee D P, Book W J (1995) Filtering micro-manipulator wrist commands to prevent flexible base motion. In: *Proceedings of American Control Conference*
12. Oppenheim A V, Schaffer R W, Buck J R (1989) *Discrete-Time Signal Processing*. Prentice-Hall, upper Saddle River, NJ
13. Oustaloup A, Moreau X, Nouillant M (1997) From fractal robustness to non-integer approach in vibration insulation: the crone suspension. In: *Proceedings of the 36th Conference on Decision & Control*. San Diego, California, USA.
14. Podlubny I (2002) Geometrical and physical interpretation of fractional integration and fractional differentiation. *Journal of Fractional Calculus & Applied Analysis* 5(4): 357–366

15. Singer N C, Seering W P (1988) Using acausal shaping techniques to reduce robot vibration. In: Proceedings of the IEEE International Conference on Robotics & Automation. Philadelphia PA, USA.
16. Yoshikawa T, Hosoda K, Doi T, Murakami H (1993) Quasi-static trajectory tracking control of flexible manipulator by macro-micro manipulator system. In: Proceedings of the IEEE International Conference on Robotics & Automation, Atlanta, GA, USA, pp 210–215